

## Ionization of H and He<sup>+</sup> by electrons and positrons colliding at near-threshold energies

A. E. Wetmore and R. E. Olson

*Physics Department and Laboratory for Atomic and Molecular Research, University of Missouri—Rolla,  
Rolla, Missouri 65401*

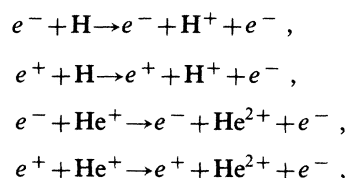
(Received 21 April 1986)

Ionization cross sections for the four combinations of electrons and positrons on H and He<sup>+</sup> have been calculated at energies near the threshold for ionization using the classical trajectory Monte Carlo method. In addition, charge-exchange (positronium formation) cross sections have been calculated for the positron-impact collisions. The ionization cross sections compare well with the predictions of the Wannier and Klar models and experimental observations. Our results indicate that the Wannier-type threshold behavior may extend to higher energies than was previously thought. In addition, we have calculated two of the collision parameters, the angle and the relative separation between the escaping particles, used in the Wannier and Klar models, and find good agreement with the values predicted by these theories.

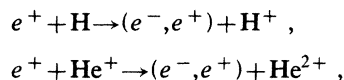
### INTRODUCTION

A recent quantum-mechanical theory by Temkin<sup>1-4</sup> suggests a form for the threshold-energy dependence of the ionization cross section which does not follow a simple power law relationship. The Coulomb-dipole interaction that Temkin assumes to be important near threshold energies leads to a modulation of the cross section which has infinitely rapid oscillations as the energy approaches threshold. These oscillations are in disagreement with the predictions of the Wannier<sup>5</sup> model which yields a simple power-law relationship. While Temkin's model appears to be applicable only to an extremely small energy range,  $E < 0.1$  eV above threshold, it has cast doubt upon the usefulness of the Wannier model.

We have examined the ionization processes



and the positronium-formation processes



near the threshold for the ionization processes.

The Wannier model is strictly classical and based on an analytical model of the ionization process. The central hypothesis is that, near threshold energies, the ionization process will be controlled by the forces acting on the electrons as they escape, i.e., the long-range Coulomb forces rather than the short-range forces. Since the long-range forces should be the controlling factors, the details of the collision during the time when the electrons are close to the nucleus should not affect the ionization cross section.

Therefore, it should be possible to ignore most quantum-mechanical effects except for exchange.

The Wannier model is completely classical. The classical trajectory Monte Carlo (CTMC) method should test the Wannier models predictions since the CTMC method is "exact" within the classical framework and includes all forces and recoil effects in a three-dimensional framework. In addition, the CTMC method gives absolute cross sections which can be compared with experimental results. This test of the absolute cross section is a very stringent requirement of the CTMC theory, and is in contrast to most analytical methods which give no absolute magnitude to the cross sections. In the case of positron-impact collisions, the CTMC method determines the positronium-formation cross section in the same calculation as the ionization cross section. Further tests we make compare the calculated values of the Wannier parameters,  $\gamma$  and  $\xi$ , to the theory's predictions. These two parameters are the angle between the particles as they escape,  $\gamma$ , and the parameter which relates the relative separation between the target nucleus and the two escaping electrons,  $\xi$ .

While the Wannier model applies only to electrons incident on hydrogenic targets, the fundamental assumptions (ionization dominated by the escape process) have been applied to positron-atom collisions by Klar.<sup>6</sup> Klar's calculations indicate that there also will be a power law form for the ionization cross section of positron-atom collisions. In the CTMC calculation we have included the charge exchange to the continuum cross section as part of the ionization cross section. The threshold region for the ionizing collisions is expected to reach to at least several eV.

In contrast to the work of Temkin<sup>2,3</sup> which predicts that ionization by positrons will follow the same type of law as the ionization by electrons, Geltman<sup>7</sup> suggests that even the form of the threshold laws will be different for the two cases. Also, he has suggested that the range of validity of the scaling relationships may be limited to 5 meV above threshold.

## CLASSICAL MODEL

In the Wannier formulation the physical coordinates used to describe the collision are  $r_1, r_2, \gamma$ , and the conjugate momenta  $p_1, p_2, p_\gamma$ . The variables subscripted 1 and 2 refer to the distance and momentum of the two electrons relative to the ionic core. The angle  $\gamma$  is the angle between the position vectors of the two electrons, and  $p_\gamma$  is the conjugate momentum of  $\gamma$ . The electron coordinates can be rewritten in terms of the hyperradius  $r$  and hyperangle  $\xi$ ,

$$r_1 = r \cos(\xi/2), \quad (1a)$$

$$r_2 = r \sin(\xi/2), \quad (1b)$$

$$0 < \xi < \pi, \quad (1c)$$

$$r^2 = r_1^2 + r_2^2. \quad (1d)$$

For electron collisions the value of  $\xi$  is a measure of the relative separation of the two electrons from the nucleus. Values of  $\xi$  near 0 or  $\pi$  correspond to a single electron escaping (elastic scattering, excitation or classical exchange). Values of  $\xi$  near  $\pi/2$  ( $r_1 = r_2$ ) correspond to ionization. The value of  $r$  is a measure of the electrons' separation from the nucleus. For ionization, we are interested in the state of the system as  $r$  tends to infinity. We use the ratio of  $r_1/r_2$  and the angle between the escaping electrons as a test to see if the ionization events that we find are "threshold" events or not.

Examples of the expected geometry for electron and positron collisions leading to ionization are shown in Figs. 1 and 2. For electron-hydrogen collisions, Fig. 1, it is expected that the dominant ionization process occurs when the incident electron and the electron originally bound to the target leave in opposite directions ( $\gamma$  is near  $\pi$ ), with the nucleus between the electrons. The case with positrons incident on the hydrogenic target is shown in Fig. 2. In this case the electron from the target stays between the positively charged ionic core and the positron. Unlike the case of electron-impact ionization the positron escapes in the same direction as the target electron ( $\gamma$  is near 0).

Wannier's analysis of electron-hydrogen collisions showed that at zero relative energy above the threshold ( $\epsilon = E - E_{\text{threshold}}$ ) the trajectories for all states leading to ionization converge to the parameters:  $\xi = \pi/2$ ,  $\gamma = \pi$ . The cross section near threshold was shown to depend on energy as

$$\sigma = A \epsilon^{(\mu/2 - 1/4)} \quad (2a)$$

with

$$\mu = \frac{1}{2} \left[ \frac{(100Z - 9)}{(4Z - 1)} \right]^{1/2}, \quad (2b)$$

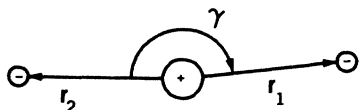


FIG. 1. A schematic representation of the geometry predicted by the Wannier theory for successful ionization by electrons.

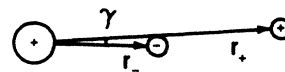


FIG. 2. A schematic representation of the geometry predicted by the Klar theory for successful ionization by positrons.

where  $Z$  is the charge of the ionic core and  $\epsilon$  is the energy above the threshold for ionization. For the two cases that we are interested in,  $Z = 1, 2$ , the exponents in the power law are 1.1269 and 1.0559. The requirement for the validity of the Wannier model is that the ratio of the collision energy minus the threshold energy divided by the charge (in atomic units) is much less than 1.0 ( $\epsilon/Z \ll 1.0$ ). For hydrogen and singly charged helium this corresponds to several eV. The Wannier, Temkin, and Klar models are all valid for  $S$ -wave scattering. In the classical trajectory Monte Carlo calculation we have not attempted to distinguish the final angular momentum states of the collisions.

## THE CLASSICAL TRAJECTORY MONTE CARLO METHOD

The use of the (CTMC) method in studying electron-impact ionization has been described by Abrines, Percival, and Valentine,<sup>8</sup> Percival<sup>9</sup>, and more recently by Dimitrijevic and Grujic.<sup>10,11</sup> Our study is similar to the work of Abrines *et al.* in that we perform a three-body three-dimensional CTMC experiment consisting of a large number (sometimes tens of thousands) of trajectories for each energy, from which we calculate a cross section. The method used by Dimitrijevic and Grujic uses a much

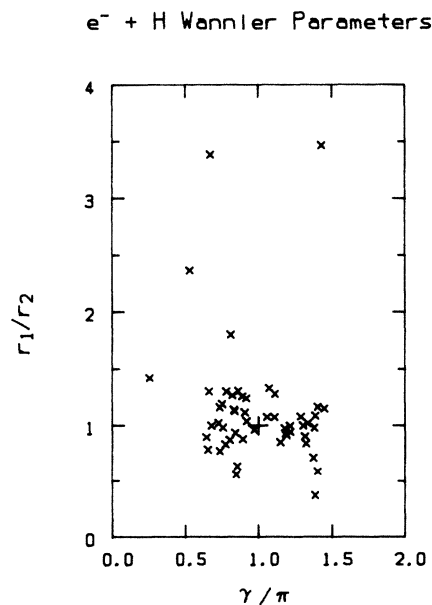


FIG. 3. A scatter diagram for the angle between the escaping electrons and the ratio of the two electron-nucleus separations. Electrons on atomic hydrogen at 14.4 eV. The points are individual ionization events from the Monte Carlo calculation.

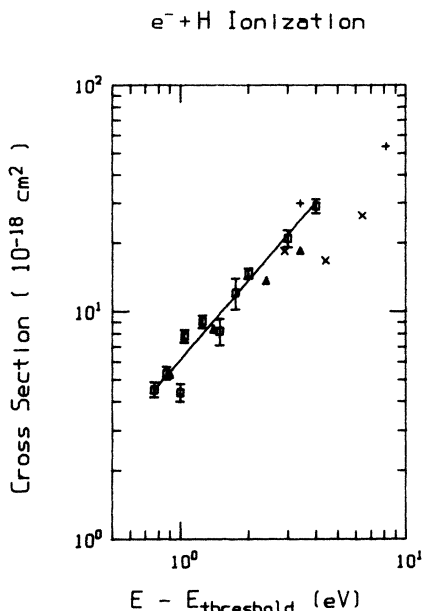


FIG. 4. The ionization cross section for electrons incident on atomic hydrogen. The energy is measured relative to the 13.6-eV threshold. The identification is  $\square$ , this work CTMC; —, fit of present results to power threshold law with fixed 13.6-eV threshold; +, Percival and Richards (Ref. 14);  $\times$ , Fite and Brackman (Ref. 13);  $\blacktriangle$ , McGowan and Clarke (Ref. 15).

smaller number of trajectories which are examined in detail to decide which portions of phase space contribute to the cross section.

In addition to calculating the cross sections and fitting these to a power threshold law, we also calculate two parameters predicted by the Klar and Wannier theories.

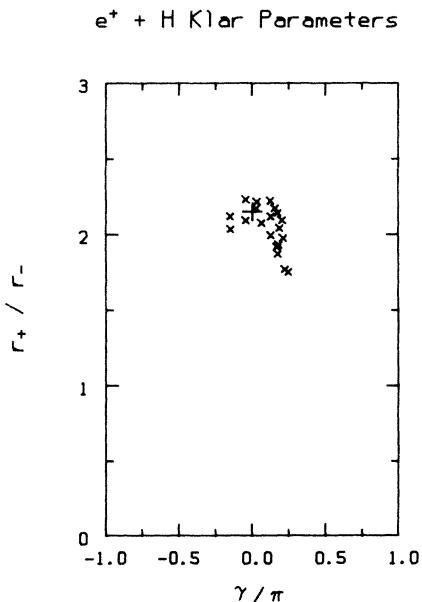


FIG. 5. A scatter diagram for the angle between the escaping electrons and the ratio of the positron-nucleus separation to electron-nucleus separation. Positrons on atomic hydrogen at 18.8 eV. The points are individual ionization events from the Monte Carlo calculation.

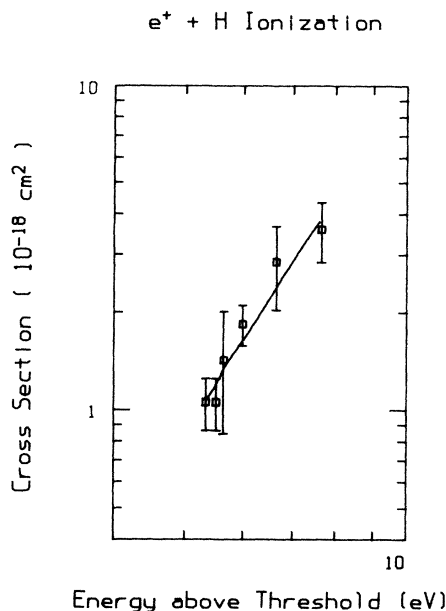


FIG. 6. The ionization cross section for positrons incident on atomic hydrogen. The energy is measured relative to 13.6-eV. The line is the power-law fit to the calculations with a fixed 13.6 eV threshold.

These parameters are the ratio of the radii (which is related to the hyperangle  $\xi$ ) and  $\gamma$ , the angle at which the particles escape. A scatter diagram which shows these parameters is included at one representative energy for each of the four collision systems. Each of the points on these diagrams is the result of a single trajectory which resulted in an ionization event being recorded by the Monte Carlo program.

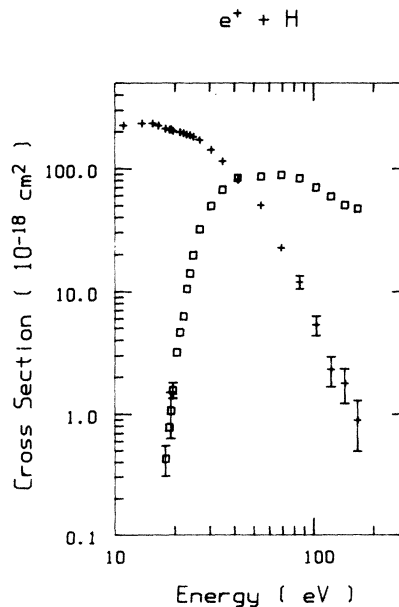


FIG. 7. The ionization,  $\square$ , and charge exchange (positronium formation), +, cross sections for positrons incident on atomic hydrogen.

TABLE I. Fitting parameters and power-law exponents for  $e^- + \text{H}$  ionization. The uncertainties are one-standard-deviation values.

Author	Threshold	Magnitude ( $10^{-18} \text{ cm}^2$ )	Exponent
This work	13.6 eV	$6.14 \pm 0.20$	$1.153 \pm 0.04$
	$13.78 \pm 0.28$ eV	$7.57 \pm 0.24$	$1.031 \pm 0.25$
Wannier (Ref. 5)			1.127
Fite and Brackman (Ref. 12)		$6.9 \pm 0.5$	1.0
Geltman (Ref. 7)		3.9	1.0
McGowan and Clarke (Ref. 13)		5.6	1.0
		5.9	1.13
Rudge and Seaton (Ref. 13)		13.6	1.0
Cvejanovic and Read $e^- + \text{He}$ (Ref. 19)			$1.131 \pm 0.019$

Thus we will be able to directly compare the results and predictions of the analytical models proposed by Klar and Wannier with "exact" three-body, three-dimensional classical calculations. The assumptions used in the analytical models can then be carefully analyzed and the cross sections can be directly compared to experimental results without resorting to any normalization procedure.



Wannier's analysis of the electron-impact ionization of atomic hydrogen yields the following results.

- (1) The angle  $\gamma$  will be  $\pi$ , i.e., the escaping electrons will leave in opposite directions.
- (2) The hyperangle  $\xi$  will be  $\pi/2$ , i.e., the ratio of the length of the electron-nucleus vectors will be 1.
- (3) The exponent in the power threshold law, Eq. (2), will be 1.127.

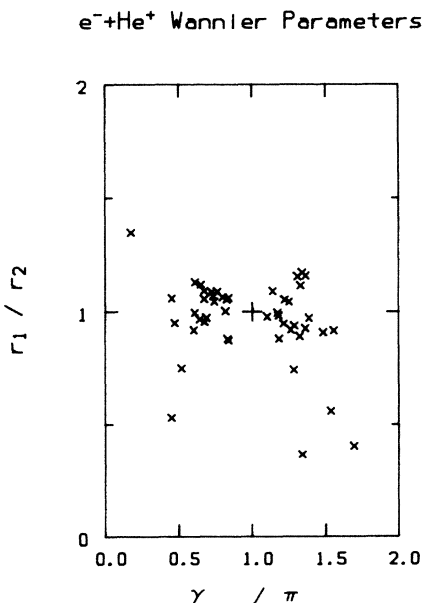


FIG. 8. A scatter diagram for the angle between the escaping electrons and the ratio of the two electron-nucleus separations. Electrons on helium plus at 57.2 eV. The points are individual ionization events from the Monte Carlo calculation.

The first two parameters are shown in Fig. 3 for an energy of 0.8 eV above threshold (14.4 eV). The data points are the results of individual ionization events. The results cluster around the marker located at 1,1 predicted by the Wannier theory. Our results also indicate that there is not an important contribution to ionization from events where  $r_1/r_2 \geq 2$ .

The cross section for ionization of H by electrons is shown in Fig. 4. The power-law fit to the data is

$$\sigma = 6.15(E - 13.6 \text{ eV})^{1.15} \times 10^{-18} \text{ cm}^2.$$

The fit was made with only two adjustable parameters, the exponent and the proportionality factor which depends on the absolute magnitude of the cross section.

The agreement with the Wannier theory is quite good. As a further test of the calculations we allowed the

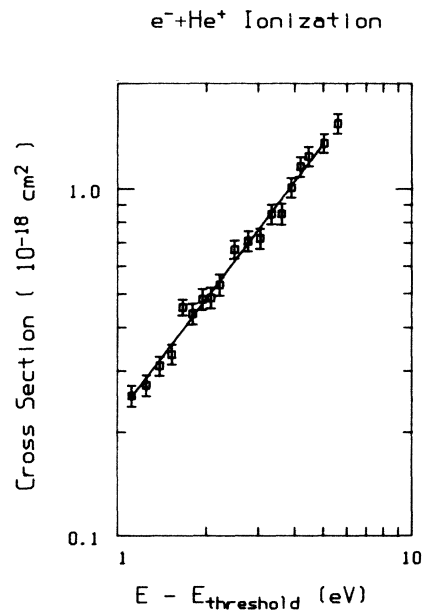


FIG. 9. The ionization cross section for electrons incident on helium plus. The energy is measured relative to the 54.4-eV threshold. The line is the power-law fit to the calculations with fixed 54.4-eV threshold.

TABLE II. Fitting parameters and power-law exponents for  $e^+ + H$  ionization. The uncertainties are one-standard-deviation values.

Author	Threshold	Magnitude ( $10^{-21} \text{ cm}^2$ )	Exponent
This work	13.6	$0.074 \pm 0.061$	$3.01 \pm 0.05$
	$14.96 \pm 0.13 \text{ eV}$	$0.219 \pm 0.018$	$3.99 \pm 0.05$
Klar (Ref. 6)			2.65

curve-fitting routine to adjust the threshold energy while fitting the data. This is a check for the existence of a valid threshold (for electrons on H the threshold should be at 13.6 eV), any variation of the threshold from its expected value is a sign we are not correctly modeling the threshold behavior or that we are too far above the threshold energy. In this case the fitted cross section was

$$\sigma = 7.57(E - 13.8 \text{ eV})^{1.03} \times 10^{-18} \text{ cm}^2.$$

A summary of these results, including uncertainties at the one-standard-deviation level, and other work is shown in Table I.

Also included in Fig. 4 are the early experimental results of Fite and Brackman,<sup>12</sup> the more recent measurements of McGowan and Clarke<sup>13</sup> and the calculations of Percival and Richards.<sup>14</sup> The Percival and Richards calculation is also a CTMC calculation; however, it was made at higher energies. Our results are in good agreement. The experimental results of McGowan and Clarke<sup>13</sup> are in excellent agreement with our absolute cross-section determination. The cross section of Fite and Brackman is approximately half the size of ours.

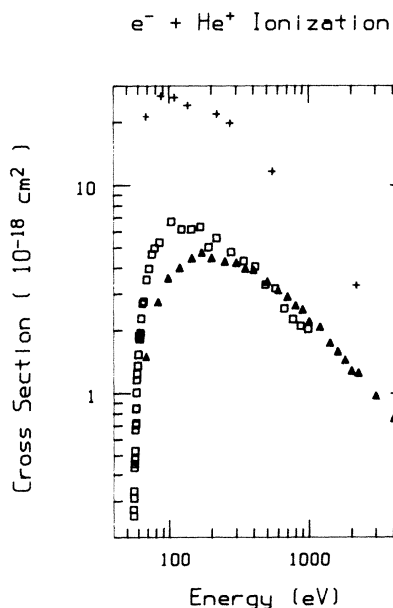


FIG. 10. The ionization cross section for electrons on helium plus. The identification is  $\square$ , current work;  $+$ , Percival and Richards (Ref. 14);  $\blacktriangle$ , Peart, Walton, and Dolder (Ref. 17).

TABLE III. Fitting parameters and power-law exponents for  $e^- + \text{He}^+$  ionization. The uncertainties are one-standard-deviation values.

Author	Threshold	Magnitude ( $10^{-19} \text{ cm}^2$ )	Exponent
This work	54.4 eV	$2.23 \pm 0.24$	$1.116 \pm 0.034$
	$54.52 \pm 0.32 \text{ eV}$	$2.50 \pm 0.07$	$1.056 \pm 0.157$
Wannier (Ref. 5)			1.0559

$e^+ + H$

For ionization by positron impact the expected results are somewhat different. The theory by Klar is based on the same assumptions as the Wannier theory; however, instead of the electron and positron escaping on opposite sides of the ion they escape in the same direction with the electron between the ion and the positron. The theory predicts that the ratio of the position vectors will be

$$\frac{r_+}{r_-} = \left( \frac{1 + \sin\phi_0}{1 - \sin\phi_0} \right)^{1/2}, \quad (3a)$$

with

$$\phi_0 = \cos^{-1} \left[ \frac{3Z - \sqrt{Z(4+Z)}}{2Z - 1} \right]. \quad (3b)$$

For the case of positrons ionizing neutral atoms this ratio, Eq. (3a), will be approximately 2.15. Figure 5 shows the parameters for successful ionization of hydrogen by positrons at 18.8 eV. The format of the plot is similar to Fig. 3. The target on the graph is located at the point where the angle between the escaping positron and electron is zero degrees, and the ratio of the positron-nucleus

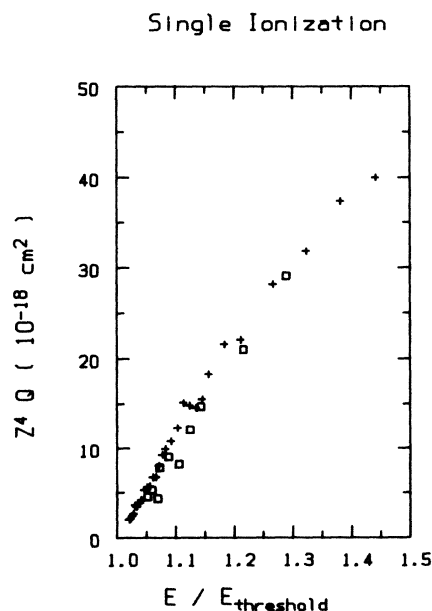


FIG. 11. Scaled cross sections comparing the  $\square$ ,  $e^- + H$ , and the  $+$ ,  $e^- + \text{He}^+$  cross sections.

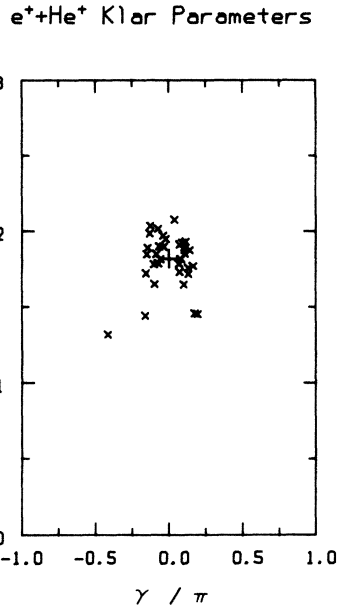


FIG. 12. A scatter diagram for the angle between the escaping electrons and the ratio of the positron-nucleus separation to electron-nucleus separation. Positrons on helium plus at 75.2 eV. The points are individual ionization events from the Monte Carlo calculation.

to electron-nucleus separation is 2.15. The data points are near the predicted value.

The cross section for ionization of H by positrons is shown in Fig. 6. The power-law fit to the data for the cross section is

$$\sigma = 7.4(E - 13.6 \text{ eV})^{3.01} \times 10^{-23} \text{ cm}^2.$$

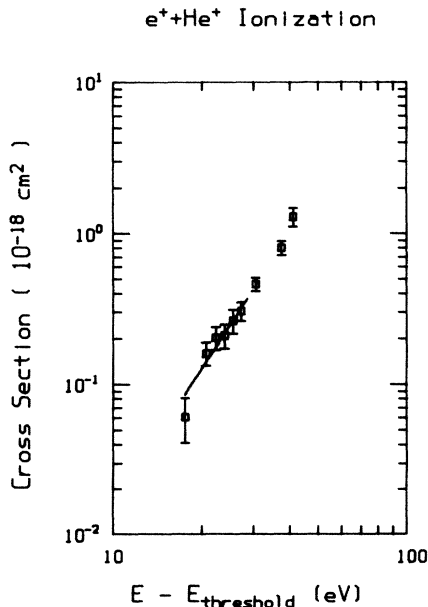


FIG. 13. The ionization cross section for positrons incident on helium plus. The energy is measured relative to 54.4 eV. The line is the power-law fit to the calculations with a fixed 54.4 eV threshold.

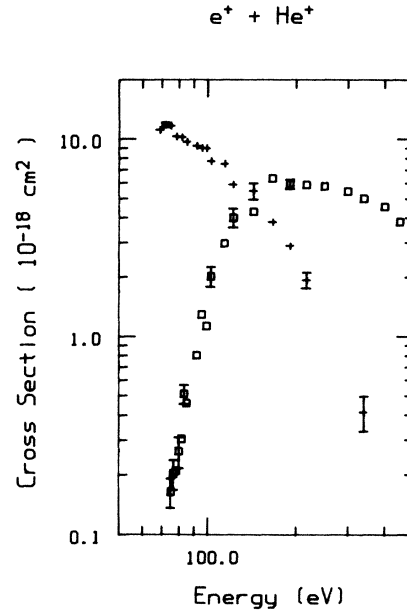


FIG. 14. The ionization,  $\square$ , and charge exchange (positronium formation),  $+$ , cross sections for positrons incident on helium plus.

This fit was made with a fixed 13.6-eV threshold energy. The power-law fit (using a variable threshold energy) to the data for the cross section is

$$\sigma = 2.2(E - 15.0 \text{ eV})^{2.81} \times 10^{-22} \text{ cm}^2.$$

These fits have an exponent which is somewhat larger than Klar's prediction of 2.65. This difference could be due to the larger energy above threshold of the positron-impact collisions relative to the electron-impact collisions and the large statistical errors in the cross sections. The calculations of  $\text{H}^+ + \text{H}$  ionization cross sections by SethuRaman, Thorson, and Lebeda,<sup>15</sup> which fit a power threshold law with an exponent of 3.0, suggest that this value of an exponent is not unreasonable for ionization near threshold energies. The ionization and charge-exchange (positronium formation) cross sections for  $e^+ + \text{H}$  over a wider energy range are displayed in Fig. 7. These results are in agreement with the calculations of Watanabe *et al.*<sup>16</sup> A summary of these results is given in Table II. In this case there are not any experimental data to compare to.

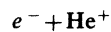
Geltman,<sup>7</sup> using the Coulomb-Born approximation for both electron and positron impact ionization, concludes

TABLE IV. Fitting parameters and power-law exponents for  $e^+ + \text{He}^+$  ionization. The uncertainties are one-standard-deviation values.

Author	Threshold	Magnitude ( $10^{-21} \text{ cm}^2$ )	Exponent
This work	54.4 eV	$1.63 \pm 0.12$	$2.988 \pm 0.023$
	$55.09 \pm 0.56$ eV	$1.74 \pm 0.13$	$2.994 \pm 0.024$
Grujic (Ref. 19)			2.9737

that the energy dependence will be quite different for the two cases and suggests that, as in a Wigner two-body threshold process, the energy range of the threshold process may be limited to 5 meV. The ionization laws which are described in Geltman's work are not intended to be rigorous, but to illuminate the qualitatively different behavior for the two cases.

Another factor which reduces the rigor of our test is the energy above threshold. In the  $e^- + \text{H}$  case we made calculations extending to less than 1 eV above the threshold. The  $e^+ + \text{H}$  calculations were only able to reach approximately 5 eV above threshold. The reason we are not able to extend the positron ionization calculations to lower energy is that the positronium-formation cross section, which is an integral part of the CTMC calculation, becomes an overwhelming process which greatly complicates any theoretical analysis.



The Wannier analysis of the electron-impact ionization of  $\text{He}^+$  yields much the same results as for ionization of hydrogen. The major difference is that the exponent predicted from Eq. (2) will be 1.056.

The angle  $\gamma$  and the ratio of the electron-nucleus separation at 57.2 eV (2.8 eV above threshold) are shown in Fig. 8. As in Fig. 3 the data points are the results of individual ionization events. The results do not agree with the predictions as well as the data from the hydrogen ionization, probably reflecting the fact that we are 2.8 eV removed from the threshold energy.

The cross section for ionization of  $\text{He}^+$  by electrons is shown in Fig. 9. The power-law fit to the data is

$$\sigma = 2.23(E - 54.4 \text{ eV})^{1.12} \times 10^{-19} \text{ cm}^2.$$

Again the fit was made with only two adjustable parameters.

The agreement with the Wannier theory is quite good. When we allowed the curve fitting routine to adjust the threshold energy while fitting the data we obtained the following fit:

$$\sigma = 2.50(E - 54.5 \text{ eV})^{1.06} \times 10^{-19} \text{ cm}^2.$$

These results are summarized in Table III.

Figure 10 shows the electron ionization of singly charged helium over a wider energy range and includes the erroneous results of Percival and Richards.<sup>14</sup> Also shown are the experimental data of Peart, Walton, and Dolder.<sup>17</sup> The cross sections of Percival and Richards are roughly four times the size of our current results. The experimental results of Peart *et al.* are in very good agreement above 200 eV. Below 200 eV the peak of their cross section is 27% smaller than in our calculation and the location of the peak is at 175 eV rather than 100 eV.

Scaled cross sections for the single ionization by electron impact on H and  $\text{He}^+$  are shown in Fig. 11. As expected the results are consistent with Thompson's scaling

of the cross sections, which predicts that the cross section times the fourth power of the ionic charge will scale with the ratio of the energy to the threshold energy.

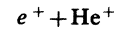


Figure 12 shows the parameters for successful ionization of singly charged helium by positrons at 72.0 eV. The format of the plot is similar to Fig. 5. As in the positron-hydrogen results, the angle between the escaping positron and electron is zero degrees, however the expected ratio of the positron-nucleus to electron-nucleus separation [Eq. (3a)] is 1.82. Again the data points are near the predicted value.

The cross section for ionization of  $\text{He}^+$  by positrons is shown in Fig. 13. The power-law fit to the data for the cross section is

$$\sigma = 1.6(E - 54.4 \text{ eV})^{2.99} \times 10^{-21} \text{ cm}^2.$$

The power-law fit using an adjustable threshold energy to fit the data is

$$\sigma = 1.7(E - 55.1 \text{ eV})^{2.99} \times 10^{-21} \text{ cm}^2.$$

A summary of these results is shown in Table IV. The theoretical value of the exponent in the power law has been given by Grujic<sup>18</sup> for the general case; for the  $\text{He}^+$  target the value is 2.9738. In Fig. 14 the ionization and charge-exchange (positronium formation) cross sections are shown.

## CONCLUSIONS

Our results indicate that in the energy range of  $1.04 < E/E_{\text{threshold}} < 1.15$  above the threshold for ionization of both H and  $\text{He}^+$  by electrons, the Wannier theory yields a valid description of the energy dependence of the ionization cross section. In addition the CTMC technique has calculated absolute cross sections that are in reasonable agreement with experimental measurements. The geometry of these ionization events is as predicted by the Wannier theory.

In the case of ionization of H and  $\text{He}^+$  by positrons, the geometry of the ionization events is similar to the theoretical predictions by Klar. Our calculations are in basic agreement with the exponent in the power-law relationship predicted by Klar. However, the small size of the ionization cross section (due to the competing positronium-formation channel) prevented us from calculating the ionization component of the electron removal cross section at energies nearer to the threshold. Absolute magnitudes for both the ionization and positronium-formation cross sections have been calculated.

## ACKNOWLEDGMENT

Work supported by the Office of Fusion Energy of the U.S. Department of Energy.

- <sup>1</sup>A. Temkin, *Comments At. Mol. Phys.* **11**, 287 (1982).  
<sup>2</sup>A. Temkin, *J. Phys. B* **15**, L301 (1982).  
<sup>3</sup>A. Temkin, *Phys. Rev. Lett.* **49**, 365 (1982).  
<sup>4</sup>A. Temkin, *Small Accelerator Conference*, Denton, TX, 1982 (unpublished).  
<sup>5</sup>G. H. Wannier, *Phys. Rev.* **90**, 817 (1953).  
<sup>6</sup>H. Klar, *J. Phys. B* **14**, 4165 (1981).  
<sup>7</sup>S. Geltman, *J. Phys. B* **16**, L525 (1983).  
<sup>8</sup>A. Abrines, I. C. Percival, and N. A. Valentine, *Proc. Phys. Soc.* **89**, 515 (1966).  
<sup>9</sup>I. C. Percival, *Comput. Phys. Commun.* **6**, 347 (1974).  
<sup>10</sup>M. S. Dimitrijevic and P. Grujic, *J. Phys. B* **16**, 297 (1983).  
<sup>11</sup>M. S. Dimitrijevic and P. V. Grujic, *J. Phys. B* **12**, 1873 (1979).  
<sup>12</sup>W. L. Fite and R. T. Brackman, *Phys. Rev.* **112**, 1141 (1958).  
<sup>13</sup>J. W. McGowan and E. M. Clarke, *Phys. Rev.* **167**, 43 (1968).  
<sup>14</sup>I. C. Percival and D. Richards, *Mon. Not. R. Astron. Soc.* **183**, 329 (1978).  
<sup>15</sup>V. SethuRaman, W. R. Thorson, and C. F. Lebeda, *Phys. Rev. A* **8**, 1316 (1973).  
<sup>16</sup>A. Ohsaki, T. Watanabe, K. N. Nakanishi, and K. Iguchi, *Phys. Rev. A* **32**, 2640 (1985).  
<sup>17</sup>B. Peart, D. S. Walton, and K. T. Dolder, *J. Phys. B* **2**, 1347 (1969).  
<sup>18</sup>P. Grujic *J. Phys. B* **15**, 1913 (1982).  
<sup>19</sup>S. Cvejanovic and F. H. Read, *J. Phys. B* **7**, 1841 (1974).